nature communications

Article

https://doi.org/10.1038/s41467-025-58316-1

Iridium porphyrin-catalysed asymmetric carbene insertion into primary N-adjacent C–H bonds with TON over 1000000

Received: 11 September 2024

Accepted: 17 March 2025

Published online: 07 April 2025

Check for updates

Zong-Rui Li[1,4], Kun Zhan[2,4], Yi-Jie Wang[1], Liang-Liang Wu[3], Guo-Lin Lu[1], Hao-Yang Wang[1], Xiao-Long Wan[1], Zhen-Jiang Xu[1] ✉, Kam-Hung Low[2] & Chi-Ming Che[1,2] ✉

Selective functionalization of ubiquitous C-H bonds in organic molecules provides a straightforward and efficient approach to construct complex molecules with fewer synthetic steps and high atom economy, thus promoting more sustainable and economical chemical synthesis. A formidable challenge in the field is to increase the turnover numbers (TONs) for catalytic C-H functionalization reactions reported in the literature (generally <10,000) to reasonably high levels to reduce the cost of the reaction. Another challenge is the selective functionalization of less reactive primary C(sp^3)-H bonds compared to other types of more reactive C-H bonds. We now demonstrate an efficient iridium porphyrin-catalysed asymmetric carbene insertion into primary N-adjacent C(sp^3)-H bond of N-methyl indoline and N-methyl aniline derivatives. Using chiral iridium porphyrin as a catalyst, chiral β-amino acid derivatives have been obtained with very high yields and excellent ee values (up to 99%), and TONs as high as 84,000 to 1,380,000. The reaction can be readily performed on a 100 g scale while retaining its high efficiency and selectivity. We also show that this iridium catalysis can efficiently access oligomers and polymers of β-amino acid derivatives via stepwise C-H insertion, demonstrating its potential applications in materials science via C-H bond functionalization reactions.

Efficient and highly selective catalytic chemical transformation reactions are the 'Holy Grail' of organic synthesis and play a pivotal role in modern society[1–3]. These reactions are crucial for efficiently producing valuable compounds with minimal waste, driving sustainable practices in the modern chemical industry. For example, transition metal-catalysed asymmetric hydrogenation reactions have revolutionised modern synthetic chemistry and have had far-reaching impacts[4,5]. This powerful synthetic approach enables stereo-selective reduction of double bonds in starting materials via hydrogenation, resulting in efficient production of value-added products. The large-scale industrial application of asymmetric hydrogenation is attributed to its exceptional attributes, including high product turnover number (TON), which is usually hundreds of thousands to millions, coupled with excellent stereo-selectivity, often in excess of 95% enantiomeric excess (ee) and high atom-economy[6–12]. Catalytic C-H bond functionalization (Fig. 1a) via C-H bond activation[13–19] or C-H bond insertion[20–24] provides a direct route to convert C-H bonds into new chemical bonds. This makes it possible to install valuable functional

[1]Shanghai-Hong Kong Joint Laboratory in Chemical Synthesis, Shanghai Institute of Organic Chemistry, Shanghai, PR China. [2]State Key Laboratory of Synthetic Chemistry, Department of Chemistry, The University of Hong Kong, Hong Kong SAR, PR China. [3]Laboratory of Beam Technology and Energy Materials, Advanced Institute of Natural Sciences, Beijing Normal University, Zhuhai, PR China. [4]These authors contributed equally: Zong-Rui Li, Kun Zhan. ✉e-mail: xuzhenjiang@sioc.ac.cn; cmche@hku.hk

https://doi.org/10.1038/s41467-025-58316-1

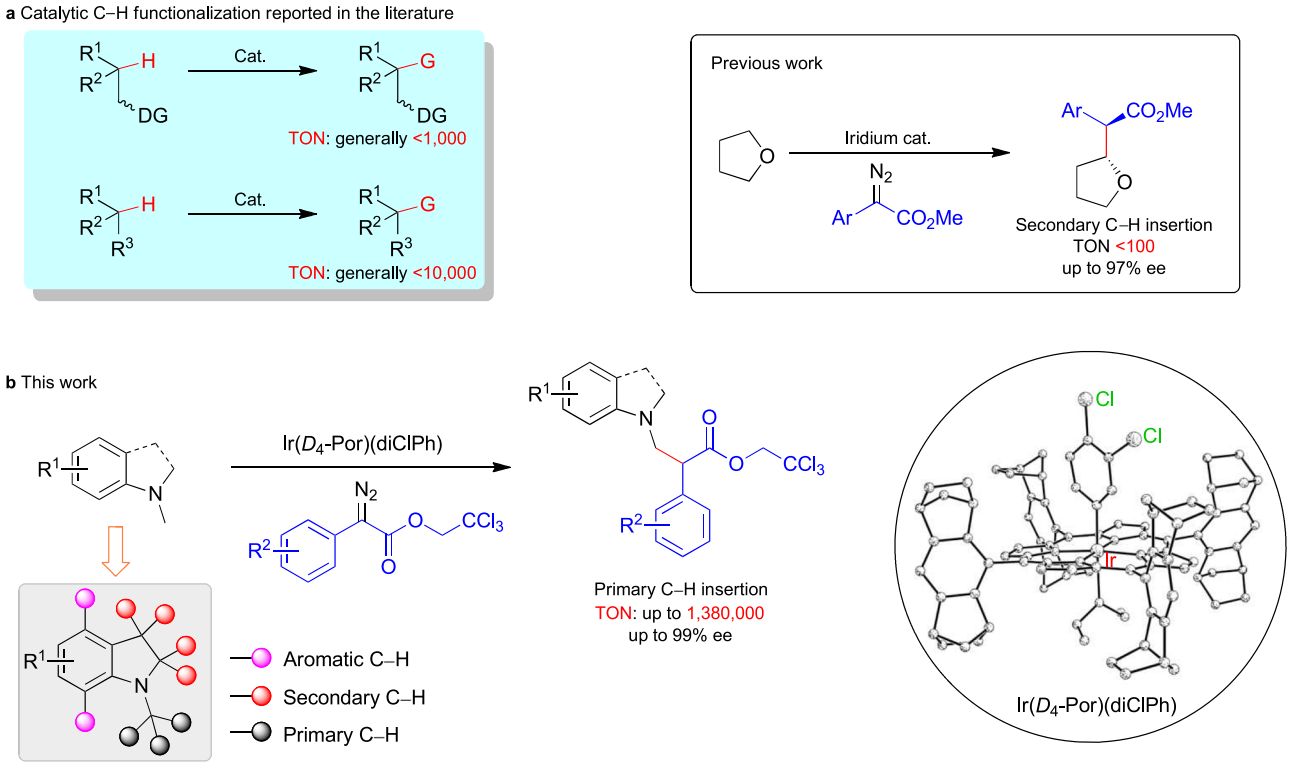

Fig. 1 | Metal-catalysed asymmetric C-H functionalization. a Functionalization of C(sp^3)-H bonds with or without directing groups (DG). Inset: our previous work. **b** Ir-catalysed carbene insertion into primary C(sp^3)-H bonds in this work.

groups and complex moieties in target molecules. Given the ubiquity of C-H bonds in organic molecules, this method provides a direct and efficient way to construct complex molecules with fewer synthetic steps and higher atom economy, thus facilitating more sustainable and economical chemical synthesis. In this regard, catalytic C-H bond functionalization has garnered widespread attention and there has been much effort devoted to its application in late-stage modification of complex molecules[14,25–27]. Transition-metal-catalysed asymmetric carbene insertions into C-H bonds with site- and stereo-selectivity offer an attractive and direct approach to this field. It is worth noting that most of the selective carbene C-H insertion reactions reported so far rely on dirhodium catalysis, through the combination of different chiral rhodium catalysts and carbene precursors. On the other hand, there are few examples of using other transition metal catalysts[14,20–23].

Despite significant advances in catalytic C-H functionalization, there are still some key challenges that need to be resolved before further large-scale applications. A particularly pressing issue in this area is how to improve the relatively low product TON in reported examples[28–35] (generally <10,000; 98,000 in one example[36]) to reasonable high levels to reduce reaction costs while minimising the impact of catalyst contamination on product. The second challenge is to selectively functionalise specific C-H bonds in target molecules that have multiple C-H bonds of similar reactivity[28,37], as well as primary C(sp^3)-H bonds that are less reactive relative to other more reactive C-H bonds[38,39].

Natural enzymes have a remarkable ability to catalyse C-H functionalization of specific substrates under mild conditions, with high activity and selectivity[40,41]. However, the difficulty in obtaining natural enzymes in large quantities means that they are generally expensive and not widely available[42–44]. In addition, the substrate scope of enzymatic reactions is often limited, and the catalytic results are sensitive to multiple factors such as pH and temperature. To address these challenges, various bio-mimetic metal complexes have been developed to catalyse C-H functionalization. Although the complexes reported so far are easier to prepare and modify than natural enzymes, their activity and selectivity are often difficult to match the efficiency of natural enzymes. Therefore, the development of robust metal catalysts that can efficiently and selectively catalyse C-H functionalization over a wide range of substrates is beneficial for unlocking the practical and large-scale application of C-H functionalization reactions in precision organic synthesis. Previously, we demonstrated that chiral iridium porphyrins can catalyse asymmetric intermolecular carbene insertions into O-adjacent secondary C-H bonds in tetrahydrofuran using donor-acceptor diazo compounds as carbene precursors[45,46] (Fig. 1a, inset). Here, we report an efficient iridium porphyrin-catalysed asymmetric carbene insertion into primary N-adjacent C(sp^3)-H bonds of N-methyl indoline and N-methyl aniline derivatives. Using chiral iridium porphyrin as a catalyst, chiral β-amino acid derivatives were obtained with very high yields and excellent ee values, with product TONs ranging from 84,000 to 1,380,000 (Fig. 1b). Notably, the reaction can be easily carried out on a 100 g scale while retaining its high efficiency and selectivity. In addition, this iridium catalysis can efficiently produce oligomers and polymers of β-amino acid derivatives through stepwise C-H insertion, demonstrating its potential application in materials science through C-H bond functionalization reactions.

Results and discussion

Carbene insertion into C(sp^3)-H bonds of N-methyl indolines

Iridium porphyrin catalysis was initiated by exploring the catalytic carbene insertion of N-methyl indoline **1a**, which has three types of C-H bonds susceptible to carbene insertion: N-adjacent primary and secondary C(sp^3)-H bonds, as well as the aryl C(sp^2)-H bonds. Notably, under common conditions, primary C-H insertion is preferred among these options (Supplementary Tables 1 and 2). Using the donor-acceptor diazo compound **2a** as the carbene precursor, rapid screening studies show that iridium porphyrin complexes can selectively afford the primary C-H insertion product **3a** (Supplementary Table 1). Encouraged by this result, chiral iridium porphyrin complexes were

used as catalysts in the reaction. To our delight, 0.5 mol% of Ir(D_4-Por)(CO)Cl proved sufficient to carry out the reaction and the desired primary C(sp^3)-H insertion product **3a** was obtained in 70% NMR yield and 97% ee, and the double insertion product **6** was obtained in 16% NMR yield within 24 h (Supplementary Table 2, entry 1). As expected, Ir(D_4-Por)Me with an axial methyl group, showed significantly higher activity due to the strong trans effect of the methyl group, resulting in the reaction being completed within 5 min; the NMR yield of **3a** was 67%, although the ee value of 90% is slightly lower (Supplementary Table 2, entry 2). Interestingly, we serendipitously discovered that a simple modification of the separation procedure in the preparation of the iridium porphyrin catalyst could significantly improve the catalytic reaction (with Ir(D_4-Por)(CO)Cl catalyst), thereby reducing the reaction time from 24 h to 2 h (Supplementary Table 2, entry 3). The 'activated Ir(D_4-Por)(CO)Cl' was compared with normal Ir(D_4-Por)(CO)Cl by various analytical methods, and no significant difference was found between the two. This suggests that the 'activated Ir(D_4-Por)(CO)Cl' may contain trace amounts of 'highly active iridium porphyrin species' that may be the 'actual catalyst' responsible for the observed efficient and selective catalysis of the C-H insertion reactions. In view of our previous findings that axial ligands may have a significant effect on the catalytic activity of metalloporphyrin-catalysed reactions[45,46], and the literature reports that iridium complexes with axial methyl[47–52] or aryl ligands[53] are highly active catalysts for carbene transfer reactions, we hypothesised that trace amounts of 'highly reactive iridium porphyrin species' may be formed during the preparation of Ir(D_4-Por)(CO)Cl in 1,2,4-trichlorobenzene. To test our hypothesis, we successfully synthesised the axially arylated iridium porphyrin Ir(D_4-Por)(diClPh) (diClPh = 3,4-dichlorophenyl) and confirmed its structure by X-ray single crystal analysis. As expected, the complex showed high catalytic activity in promoting C-H insertion reactions to produce **3a** in moderate yields and excellent enantioselectivity (Supplementary Table 2, entries 4–5). Notably, the NMR yield of **3a** increased to 83% by reducing the amount of diazo compound used to suppress the formation of the double insertion product (Supplementary Table 2, entry 6). In addition, the reaction showed excellent tolerance to a variety of common organic solvents, affording **3a** in moderate-to-good yields with exceptional enantioselectivity (Supplementary Table 2, entries 7–15). Among the solvents examined, cyclohexane and chloroform performed the best in terms of product yield and enantioselectivity. Strikingly, optimisation of the catalytic reaction by reducing the amount of catalyst (Supplementary Table 2, entries 16–22) showed that, with the use of 0.0004 mol% (4 ppm) Ir(D_4-Por)(diClPh) catalyst in cyclohexane at 40 °C and acetic acid as additive, 70% isolated yield, 96% ee and a high product TON of 175,000 were obtained for **3a** despite the longer reaction time (Supplementary Table 2, entry 22). The high activity of Ir(D_4-Por)(diClPh) is attributable to the strong trans effect of a phenyl group, coupled with introduction of two electron-withdrawing chloro-substituents on the phenyl group, which enhances the electrophilicity of the carbene group. Moreover, the large steric hindrance of diClPh combined with the chiral pocket structure of D_4-Por may better protect the catalytic centre and greatly improve the stability of the catalyst. We speculate that this interplay of electronic and steric effects enables Ir(D_4-Por)(diClPh) to efficiently catalyse asymmetric C-H insertion reactions even at very low catalyst loading.

Under optimised reaction conditions, the asymmetric C-H insertion reaction of various N-methyl indoline derivatives and donor-acceptor diazo compounds was investigated; the corresponding products are shown in Fig. 2. Highly efficient and selective primary C-H insertion of various substituted N-methyl indoline derivatives was achieved; the corresponding insertion products were obtained with good-to-excellent isolated yields (66–93%), excellent enantioselectivities (90–96% ee), and very high product TONs (88,000–330,000) (Figs. 2, 3a–g). Interestingly, this reaction is sensitive to the steric hindrance of N-methyl indoline and no primary C-H bond insertion reaction was detected for 7-bromo substituted N-methyl indoline **1 h** (Figs. 2, 3h). This reaction tolerates a range of different substituted donor-acceptor diazo compounds, and provides the corresponding insertion products (**3i**-**3m**) in moderate-to-good yields (60–90%) with excellent enantioselectivities (93–96%) and high TON from 60,000 to 226,000. Similar steric hindrance sensitivity was also observed when *o*-bromo substituted diazo compounds were used as the carbene source, and the desired insertion product **3n** was not detected in the reaction. N-Methyl tetrahydroquinoline also reacts to form **3o**, with a yield of 82%, an ee value of 94% and a TON of up to 205,000. The reaction of N-methyl benzomorpholine was also successful, providing the desired insertion product **3p** in 84% yield and 89% ee with a TON of 84,000.

Carbene insertion into C(sp^3)-H bonds of N-methyl anilines

Subsequently, the reaction was extended to various N-methyl aniline derivatives using the donor-acceptor diazo compound **2a** as carbene source, and the results are summarised in Fig. 3. Compared to N-methyl indoline, N,N-dimethyl aniline showed higher reactivity; product **8a** was formed in 85% yield and 90% ee with a TON of 428,000. Fluoro substituted N,N-dimethyl aniline derivatives showed high reactivity in the reaction, and the corresponding insertion products **8b**-**8d** were obtained in good yields (60–83%), with excellent enantioselectivity (93–99% ee) and high product TONs (600,000–1,380,000). To our knowledge, this is the highest TON reported to date for a C-H insertion reaction. N,N-Dimethyl aniline with Cl, Br, methyl or ester group on the phenyl ring was also found to be a suitable substrate in the reaction, and the corresponding primary C-H insertion products **8e**-**8i** were obtained in high yields (81–94%), excellent enantioselectivity (89–94% ee) and high TON of 207,000–236,000. N-Ethyl, benzyl or ethyl acetates were also well tolerated in the reaction and afforded **8j**-**8l** with high efficiency and selectivity. Interestingly, when **7k** with a benzyl substituent was used as substrate, the more reactive secondary benzylic C-H bond remained intact, and the desired N-methyl insertion product **8k** was obtained in 80% yield and 95% ee; this further demonstrated the high selectivity of this iridium catalysis. The reaction can be extended to N,N-dimethyl aminonaphthalene and affords **8m** and **8n** in moderate-to-good yields and good-to-high enantioselectivities. It is worth noting that methyl substituted diazo compounds, such as methyl 2-(4-bromophenyl)-2-diazoacetate, are also suitable for this reaction; compound **8o** was obtained with a yield of 80% and an ee of 89% with a TON of 267,000. These values for compound **8o** are lower than those for **8a** obtained using the 2,2,2-trichloroethyl substituted counterpart **2a**. This is consistent with previous report that 2,2,2-trichloroethyl aryldiazo-acetates outperform their methyl counterparts in metal-catalysed carbene C–H insertion reactions[54].

We also explored the reactivity of several amine-substituted pyridine compounds, including dimethylaminopyridine (DMAP) and its derivatives. Using 4-DMAP or its N-oxide as substrate, no desired insertion products **8p** or **8q** were detected (Supplementary Fig. 1). This is attributed to the coordination of the pyridine or N-oxide groups to the catalyst Ir(D_4-Por)(diClPh), which prevents the formation of the corresponding metal-carbene intermediate required for the C-H insertion reaction. We then used sterically hindered 4- or 2-DMAP derivatives as substrates to mitigate the pyridine coordination; the corresponding reactions gave C-H insertion products **8r** and **8s** with 80% ee (40% yield) and 94% ee (69% yield), respectively, despite the higher catalyst loading (1 mol%) (Supplementary Fig. 1).

The Ir(D_4-Por)(diClPh)-catalysed highly enantioselective primary C(sp^3)–H insertion reaction of N-methyl indolines and N-methyl anilines (Figs. 2 and 3) is significantly different from the non-porphyrin metal-catalysed reaction between N,N-dialkyl aniline and diazo compounds reported in the literature; the latter was found to lead to the insertion of carbene into aryl C(sp^2)-H bonds (TONs: <100)[55–57]. For the cytochrome P411 enzyme- or chiral Ir(Por)(CO)(Cl)-catalysed primary

https://doi.org/10.1038/s41467-025-58316-1

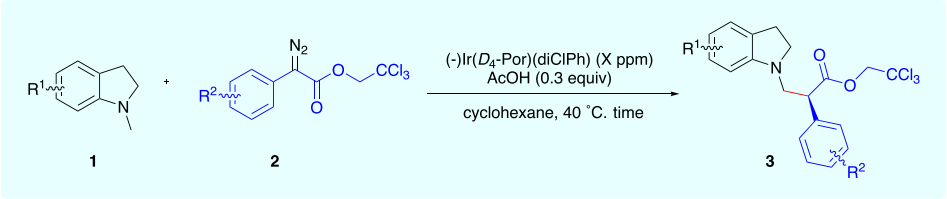

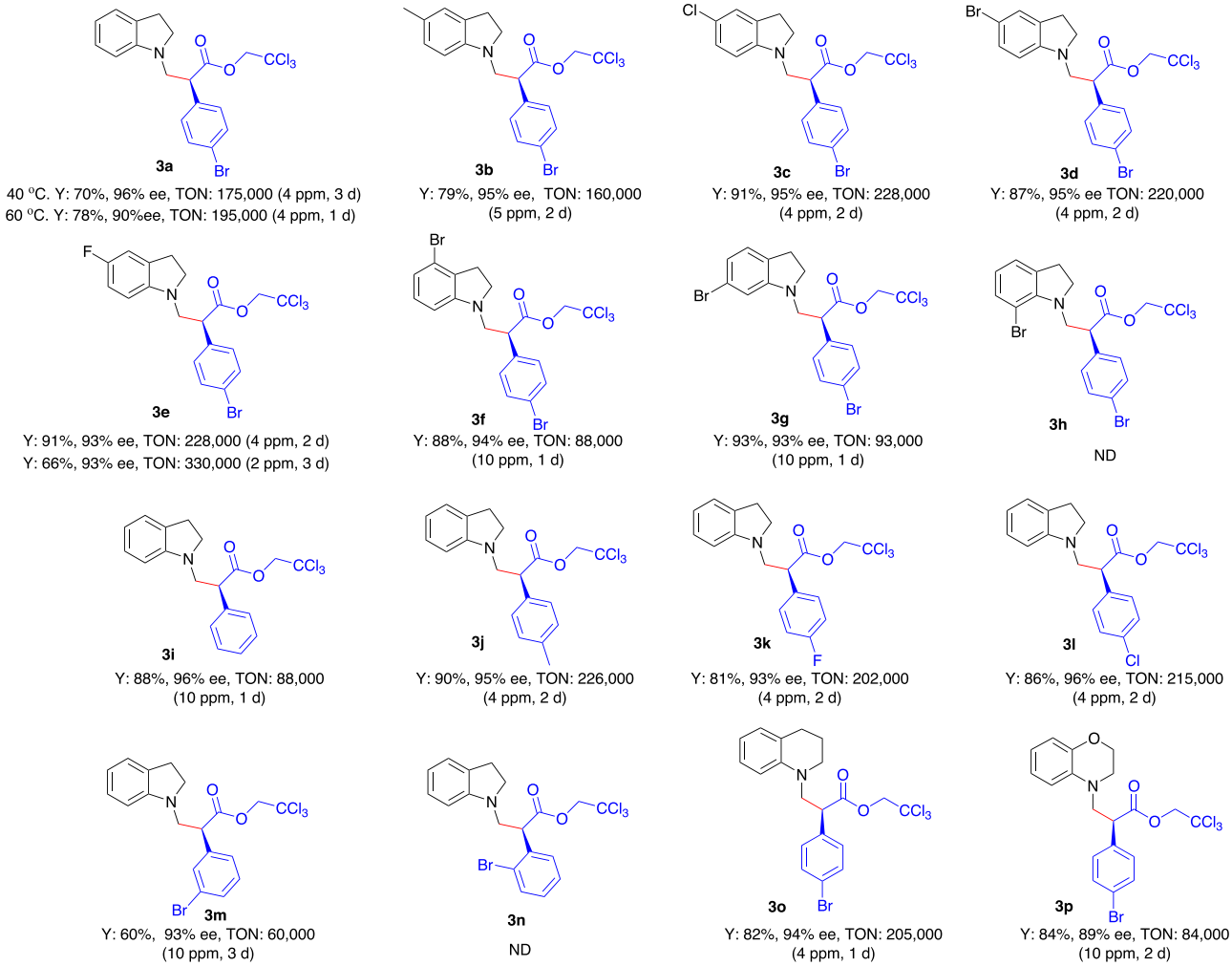

Fig. 2 | Scope of N-methyl indoline and donor-acceptor diazo compounds. The reactions were conducted in cyclohexane at 40 °C in the presence of iridium porphyrin catalyst (-)Ir(D_4-Por)(diClPh). Results for the reaction of **1a** and **2a** catalysed by (-)Ir(D_4-Por)(diClPh) at 60 °C are also shown.

C(sp^3)–H insertion of N,N-dialkyl anilines using diazo compounds, the TON was as high as 2330[40] or <100[58], respectively. There is also a report on the metal-catalysed reactions of N,N-dialkyl anilines and N-alkyl indolines with TrocNHTs, leading to the insertion of nitrenes into primary C(sp^3)–H bonds, giving products with TON of <20[59].

Large scale reactions

To further demonstrate the high efficiency of this iridium catalysed asymmetric primary C(sp^3)-H insertion reaction, two 100-gram scale reactions were performed (Fig. 4a). The reaction of N-methyl indoline **1a** and diazo compound **2a** can also proceed smoothly in cyclohexane in the presence of 4 ppm (-)Ir(D_4-Por)(diClPh) at 40 °C; the desired insertion product was obtained in 96% ee, 71% isolated yield and 177,500 TON. Similarly, *p*-fluoro-N-dimethylaniline **7b** reacted smoothly with **2a** in the presence of 1 ppm (-)Ir(D_4-Por)(diClPh) to give **8b**, with an isolation yield of 90% (equivalent to 900,000 TON) and an enantioselectivity of 93% ee. Notably, the large-scale reaction is easy to perform and maintains high efficiency and selectivity, which is of great value for potential practical applications.

Applications in organic synthesis

The insertion product **3a** could be easily converted into other valuable compounds (Fig. 4b). After treatment of DDQ, the corresponding dehydrogenated product **9** was obtained in 88% yield and 94% ee. When compound **3a** was treated with excess Zn in acetic acid, chiral acid **10** could be obtained in 68% yield, which was further converted into chiral amides **11** and **12**. When **10** was treated with N-hydroxyphthalimide, **13** was obtained in 83% yield. The absolute structure of **13** was determined to be *S* via single crystal X-ray structure analysis and the structures of the other products were assigned accordingly.

This iridium catalysis can be easily used for late-stage modification of complex molecules (Fig. 4c). When estrone derivative **14** was treated with **2a** in the presence of iridium porphyrin catalyst, the corresponding insertion product could be obtained in high yield.

https://doi.org/10.1038/s41467-025-58316-1

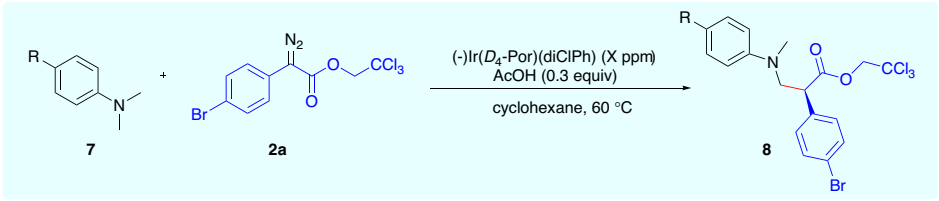

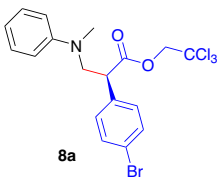

Y: 85%, 90% ee, TON: 428,000
(2 ppm, 3 d)

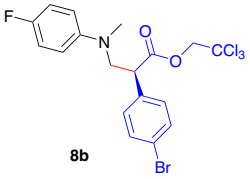

Y: 83%, 93% ee, TON: 1,190,000 (0.7 ppm, 2 d)
Y: 69%, 93% ee, TON: 1,380,000 (0.5 ppm, 3 d)

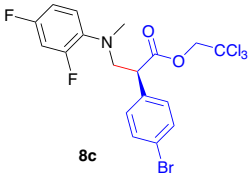

Y: 61.%, 94% ee, TON: 610,000
(1 ppm, 1 d)

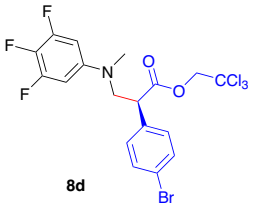

Y: 60%, 99% ee, TON: 600,000
(1 ppm, 1 d)

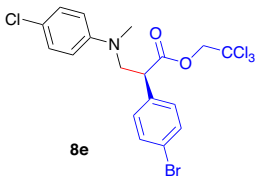

Y: 81%, 91% ee, TON: 207,000
(4 ppm, 1 d)

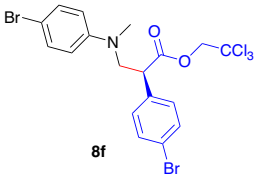

Y: 90%, 93% ee, TON: 225,000
(4 ppm, 1 d)

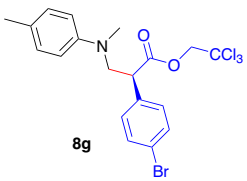

Y: 88%, 91% ee, TON: 220,000
(4 ppm, 1 d)

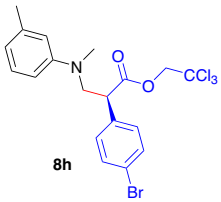

Y: 87%, 89% ee, TON: 218,000
(4 ppm, 1 d)

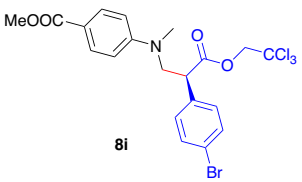

Y: 94%, 94% ee, TON: 236,000
(4 ppm, 1 d)

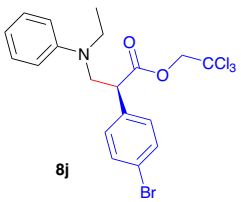

Y: 75%, 90% ee, TON: 376,000
(2 ppm, 3 d)

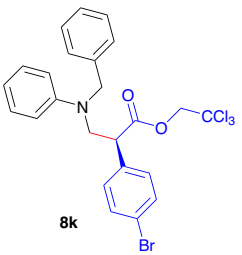

Y: 80%, 95% ee, TON: 80,000
(10 ppm, 1 d)

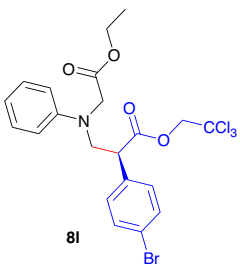

Y: 77%, 91% ee, TON: 385,000
(2 ppm, 2 d)

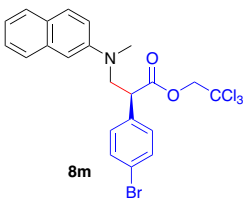

Y: 68%, 90% ee, TON: 344,000
(2 ppm, 2 d)

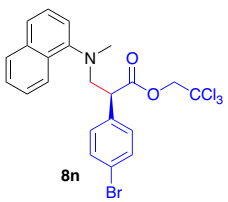

40 °C: Y: 85%, 88% ee, TON: 85,000 (10 ppm, 1 d)
60 °C: Y: 84%, 76% ee, TON: 168,000 (5 ppm, 1 d)

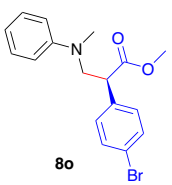

Y: 80%, 89% ee, TON: 267,000
(3 ppm, 1 d)

Fig. 3 | Scope of *N*-methyl aniline derivatives. For the reaction producing **8o**, methyl 2-(4-bromophenyl)−2-diazoacetate, instead of 2,2,2-trichloroethyl 2-(4-bromophenyl)−2-diazoacetate (**2a**), was used.

Notably, no competitive O–H insertion products were detected in the reaction, and the absolute structure of the insertion product can be fully controlled by the chiral catalyst to selectively and exclusively provide **15** or **16** with high efficiency (Fig. 4c). Subsequently, dihydroartemisinin derived substrate **17** was also tested in the reaction, and the desired C–H insertion product **18** was obtained with high efficiency and selectivity, retaining the chemically sensitive peroxide bridge motif (Supplementary Fig. 2).

Application in polymerisation reactions

Inspired by the high efficiency and selectivity of chiral iridium porphyrin in catalysing asymmetric carbene insertion of N-methyl anilines, we set out to try polymerisation reaction via sequential stepwise intermolecular carbene insertion of C–H bonds, which is a challenging task. Although the participation of carbenes in polymerisation reactions through X–H insertion (X = N, O) has been reported, to the best of our knowledge, the corresponding C–H insertion examples have not been reported. This may be attributed to the high barrier for C–H bond activation/insertion. In this regard, compound **19** bearing both the donor-acceptor diazo and N,N-dimethyl aniline moieties was designed and synthesised. To our delight, when **19** was treated with an iridium porphyrin catalyst, the polymerisation reaction proceeded smoothly to produce oligomers or polymers of amino acid ester derivatives under mild conditions (Supplementary Fig. 3). When cyclohexane was

https://doi.org/10.1038/s41467-025-58316-1

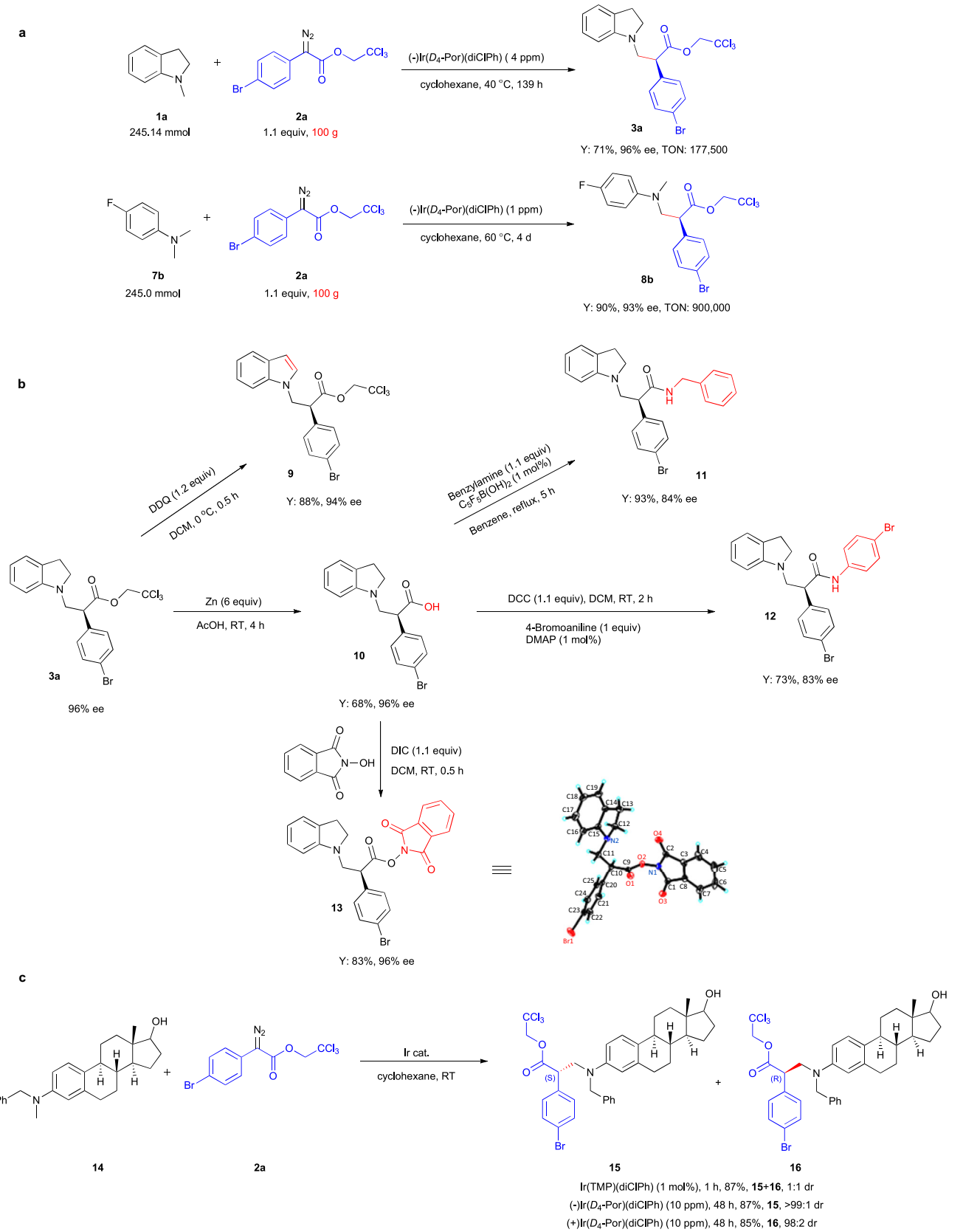

Fig. 4 | Large scale reactions and various applications. a 100-gram scale reactions. **b** Transformation reactions of **3a**. **c** Application in late-stage modification of complex bioactive compounds.

https://doi.org/10.1038/s41467-025-58316-1

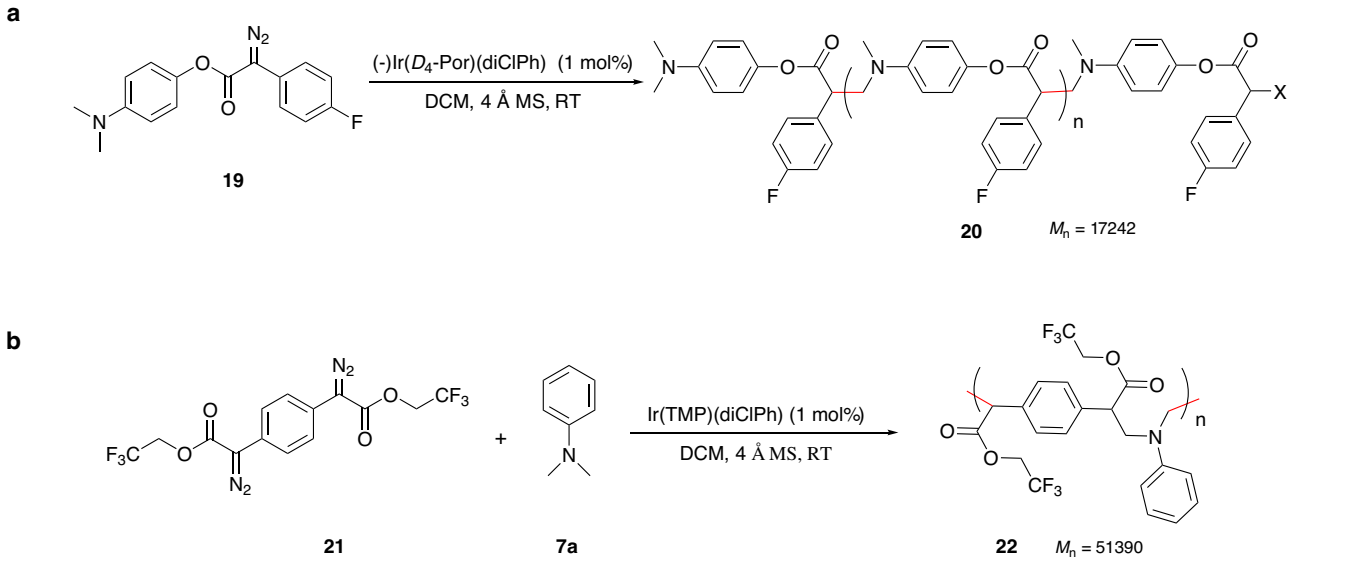

Fig. 5 | Iridium porphyrin-catalysed polymerisation reactions. a polymerisation of diazo **19**. **b** polymerisation of bisdiazo **21** with **7a**.

used as a solvent, **20** (probably due to its low solubility in cyclohexane) was obtained as an oligomer through which up to 7 units were linked. Strikingly, the use of Ir(TMP)(diClPh) as a catalyst in DCM gave **20** with a *M*n of 8375; using (-)Ir(D_4-Por)(diClPh) as a catalyst, higher *M*n values such as 17242 were obtained (Fig. 5a). This may be due to the larger steric hindrance of the D_4-Por structure, which leads to higher selectivity of the corresponding iridium carbene intermediate. Subsequently, the polymerisation reaction of the bisdiazo compound **21** with N,N-dimethyl aniline **7a** in the presence of iridium catalyst was studied. The reaction proceeded smoothly to afford polymer **22** with a M_n of 51390 (Fig. 5b) via a double C-H insertion mode. These results demonstrated that by combining robust and selective iridium catalyst with carefully designed substrates, C-H insertion reactions can serve as powerful tools for polymerisation reactions, opening another door for the development of synthetic methods for polymer chemistry.

Mechanistic studies

To elucidate the reaction mechanism, deuterated N-methyl indoline **23** was employed as the substrate; the isolated yield of corresponding deuterated product **24** was 68% and the ee was 96% (Supplementary Fig. 4a). When equal amounts of **1a** and **23** were reacted with **2a** in the presence of (-)Ir(D_4-Por)(diClPh), a mixture of **3a** and **24** was with a k_H/k_D value of 3.54 (Supplementary Fig. 4b), thus indicating that the insertion step can be rate-determining step. When 5 equivalents of TEMPO were added to the reaction mixture, **3a** could still be obtained in 61% yield and 96% ee (Supplementary Fig. 4c), so the radical pathway may not be involved in the reaction.

DFT calculations

DFT calculations were performed to give an energy landscape of the catalytic reaction, providing more insight into the unusual selectivity and the results are summarised in Fig. 6. Using the donor-acceptor diazo compound **2a** as the carbene source, an Ir-carbene intermediate (**Int2**) with axial diClPh group was formed. The Gibbs free energy of activation ($\Delta G^{\ddagger}$) is 14.6 kcal/mol, and the relative Gibbs free energy of **Int2** is -21.6 kcal/mol. **Int2** exists as a singlet Ir-carbene, and the energy of its corresponding triplet Ir-carbene is 13.3 kcal/mol higher. Using N-methyl indoline **1a** as substrate, the calculation results show that primary C(sp^3)-H can be easily activated by **Int2** with a barrier of 5.3 kcal/mol (**TS2**) in a concerted insertion manner, giving **3a** as the major product. For the generation of its enantiomer, the calculated $\Delta G^{\ddagger}$ is 8.1 kcal/mol (**TS2'**), which is higher. Based on the transition state energy difference (2.8 kcal/mol), the calculated ee is 98%, which is consistent with the experimental results. The transition states for the formation of minor products **4** and **5** (Supplementary Table 2) were also calculated. For other more feasible aromatic C(sp^2)–H bond activations to give **4**, the electrophilic addition mechanism was examined and the calculated transition state energy (**4-TS**, Fig. 6c) was 7.2 kcal/mol. However, the 2 °C-H insertion is the least favourable, with a $\Delta G^{\ddagger}$ of 8.6 kcal/mol (**5-TS**, Fig. 6c).

To better understand the energy differences of these transition states that determine the enantioselectivity and regioselectivity of the reaction, non-covalent interaction (NCI) analysis was further performed. As shown in Fig. 6, the transition state involves attractive π···π, C-H···O and C-H···π interactions as well as steric repulsion. The most favourable primary C-H activation involves (i) a strong π···π interaction between the phenyl group of the carbenoid and the aromatic ring of the indoline (3.69 Å), (ii) C-H···O (2.12 Å) interaction between the methyl group of **1a** and the carbonyl oxygen of carbenoid, and (iii) C-H···π (2.28 Å) interaction between the methyl group of **1a** and the porphyrin macrocycle. Meanwhile, the steric hindrance between **1a** and D_4-Por was determined to be minimal, as revealed by the longer H···H distances (2.12 Å and 2.30 Å). While for **TS2'**, general weak attractive interactions were calculated (π···π interaction 4.28 Å, C-H···O 2.36 Å and C-H···π 2.52 Å). In addition, the H···H distances in **TS2'** are 1.94 Å and 2.19 Å, respectively, so there is a larger steric repulsion. Therefore, both strong attractive interactions and weak repulsive steric hindrance contribute to the high enantioselectivity. For aromatic C-H activation, although the π···π distance is calculated to be 3.37 Å due to the electrophilic addition nature of the transition state, the displacement (twist) between the carbene phenyl and aromatic indoline rings reduces the overlap. Therefore, the π···π interaction is still weak. For the generation of **5**, the H···H distances in the DFT-optimised transition state structure are relatively close, 2.16 Å, 2.20 Å and 2.25 Å, respectively, which determines the steric repulsion caused by these three sites, showing that the 2° C-H insertion is the most sterically unfavourable. Overall, the primary C-H activation **TS2** is the most stable through attractive interactions and fits spatially into the catalytic pocket yielding the most prevalent product **3a**. The presence of multiple attractive NCIs synergistically lowers the activation barrier for C-H activation, making the reaction feasible and selective under mild conditions while also ensuring a high product turnover number for the catalyst.

https://doi.org/10.1038/s41467-025-58316-1

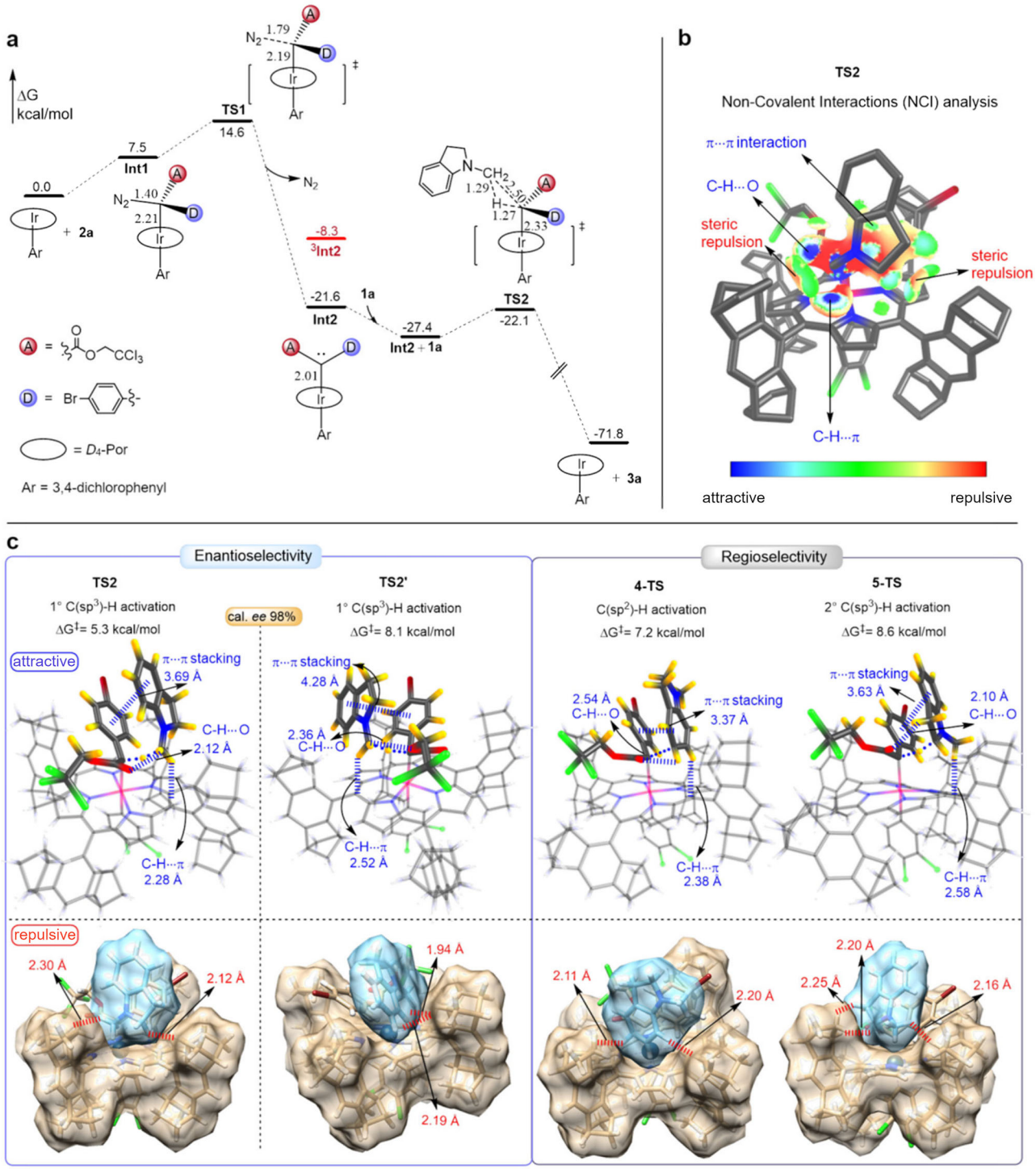

Fig. 6 | DFT calculations of reaction mechanism and selectivity. a Energy profiles of the catalytic pathway. **b** Non-covalent interaction (NCI) analysis of **TS2**. **c** Geometrical analysis of attractive and repulsive interactions in transition states that determine the selectivity. H···H distance (<2.4 Å) between the C-H of substrate (**1a**) and D_4-Por ligand in the space-filling diagrams are shown to quantitatively reveal the steric repulsion interactions.

In summary, we have developed an efficient and practical iridium porphyrin-catalysed asymmetric intermolecular primary C(sp^3)-H bond insertion reaction for a variety of N-methyl indoline and N-methyl aniline derivatives. Using ppm-level loading (-)Ir(D_4-Por) (diClPh) as the catalyst and a donor-acceptor diazo compound as the carbene source, the corresponding insertion product was obtained with high yield and excellent enantioselectivity. The product TON of 1,380,000 represents the highest TON reported to date in asymmetric C-H insertion reactions. Importantly, the insertion reaction could be easily performed on a 100-gram scale while maintaining high selectivity and efficiency. In addition, we also successfully demonstrated the promising examples of donor-acceptor diazo compound polymerisation to synthesise poly-β-aminoester through stepwise carbene insertion into primary C(sp^3)-H bonds. This result may hold promise for the development of functional polymers with a variety of applications. Overall, our results represent a significant advance in the field of C-H bond functionalization and highlight the potential of iridium porphyrin catalysis for scalable and selective synthesis of valuable chiral

compounds and for expanding the scope of C-H insertion reactions in materials science.

Methods

General procedure for carbene C–H insertion of indoline and donor-acceptor diazo compounds

Under argon protection, **1** (0.2 mmol), acetic acid (0.06 mmol, 0.3 equiv) and catalyst (4–10 ppm) were dissolved in anhydrous cyclohexane (1 mL) in a Schlenk tube, and the diazo compound **2** (0.22 mmol, 1.1 equiv.) was added into the Schlenk tube in one portion. The tube was placed in a pre-heated 40 °C oil bath and the mixture was stirred and monitored by TLC until complete consumption of **1**. The solvent was removed under reduced pressure. The desired product **3** was purified by silica gel flash column chromatography using ethyl acetate/petroleum ether (1:300 v/v) as the eluent.

General procedure for carbene C–H insertion of N-methyl aniline and donor-acceptor diazo compounds

To a solution of **7** (0.2 mmol), acetic acid (0.06 mmol, 0.3 equiv.) and catalyst (1–10 ppm) in anhydrous cyclohexane (1 mL) was added diazo compound **2** (0.22 mmol) under argon atmosphere. The reaction vessel was placed in a pre-heated 60 °C oil bath; the mixture was then stirred. The reaction was monitored by TLC until complete consumption of **7**. Solvent was removed under reduced pressure. The desired product **8** was purified by silica gel flash column chromatography using ethyl acetate/petroleum ether (1:300 v/v) as eluent.

Data availability

The authors declare that the data supporting the findings of this study, including synthetic procedures, characterisation data, further details of computational studies and NMR spectra, are available within the article and the Supplementary Information file, or from the corresponding authors upon request. The X-ray crystallographic coordinates for structures reported in this study have been deposited at the Cambridge Crystallographic Data Centre (CCDC) under deposition numbers CCDC 1976736 (for catalyst Ir(D_4-Por)(diClPh)) and CCDC2045506 (for compound **13**). These data can be obtained free of charge from The Cambridge Crystallographic Data Centre via https://www.ccdc.cam.ac.uk/structures/. Source data are provided with this paper.

References

1. Mulzer, J. Basic Principles of Asymmetric Synthesis. In *Comprehensive Asymmetric Catalysis* (eds Jacobsen, E. N., Pfaltz, A. & Yamamoto, H.) 33–100 (Springer, 1999).
2. Sethi, M. K., Chakraborty, P. & Shukla, R. Biocatalysis-A Greener Alternative in Synthetic Chemistry. In *Biocatalysis: An Industrial Perspective* (eds de Gonzalo, G. & de María, P. D.) 44–76 (RSC, 2018).
3. Beller, M. et al. Cross Coupling Reactions. In *Applied Homogeneous Catalysis with Organometallic Compounds: A Comprehensive Handbook in Four Volumes* (eds Cornils, B., Herrmann, W. A., Beller, M. & Paciello, R.) 411–464 (Wiley-VCH Verlag GmbH & Co. KGaA, 2018).
4. Magano, J. & Dunetz, J. R. Large-scale carbonyl reductions in the pharmaceutical industry. *Org. Process Res. Dev.* **16**, 1156–1184 (2012).
5. Arai, N. & Ohkuma, T. Design of molecular catalysts for achievement of high turnover number in homogeneous hydrogenation. *Chem. Rec.* **12**, 284–289 (2012).
6. Wen, J., Wang, F. & Zhang, X. Asymmetric hydrogenation catalyzed by first-row transition metal complexes. *Chem. Soc. Rev.* **50**, 3211–3237 (2021).
7. Xie, J. H., Liu, X. Y., Xie, J. B., Wang, L. X. & Zhou, Q. L. An additional coordination group leads to extremely efficient chiral iridium catalysts for asymmetric hydrogenation of ketones. *Angew. Chem. Int. Ed.* **50**, 7329–7332 (2011).
8. Yin, C. et al. A 13-million turnover-number anionic Ir-catalyst for a selective industrial route to chiral nicotine. *Nat. Commun.* **14**, 3718 (2023).
9. Doucet, H. et al. *trans*-[$RuCl_2$(phosphane)$_2$(1,2-diamine)] and chiral *trans*-[$RuCl_2$(diphosphane)(1,2-diamine)]: shelf-stable precatalysts for the rapid, productive, and stereoselective hydrogenation of ketones. *Angew. Chem. Int. Ed.* **37**, 1703–1707 (1998).
10. Ohkuma, T., Ooka, H., Hashiguchi, S., Ikariya, T. & Noyori, R. Practical enantioselective hydrogenation of aromatic ketones. *J. Am. Chem. Soc.* **117**, 2675–2676 (1995).
11. Zhao, B., Han, Z. & Ding, K. The N-H functional group in organometallic catalysis. *Angew. Chem. Int. Ed.* **52**, 4744–4788 (2013).
12. Zhang, L., Tang, Y., Han, Z. & Ding, K. Lutidine-based chiral pincer manganese catalysts for enantioselective hydrogenation of ketones. *Angew. Chem. Int. Ed.* **58**, 4973–4977 (2019).
13. Docherty, J. H. et al. Transition-metal-catalyzed C-H bond activation for the formation of C-C bonds in complex molecules. *Chem. Rev.* **123**, 7692–7760 (2023).
14. Liu, C.-X. et al. Rhodium-catalyzed asymmetric C-H functionalization reactions. *Chem. Rev.* **123**, 10079–10134 (2023).
15. Lucas, E. L. et al. Palladium-catalyzed enantioselective β-C(sp^3)-H activation reactions of aliphatic acids: a retrosynthetic surrogate for enolate alkylation and conjugate addition. *Acc. Chem. Res.* **55**, 537–550 (2022).
16. Zhang, Z., Chen, P. & Liu, G. Copper-catalyzed radical relay in C(sp^3)-H functionalization. *Chem. Soc. Rev.* **51**, 1640–1658 (2022).
17. Chan, A. Y. et al. Metallaphotoredox: the merger of photoredox and transition metal catalysis. *Chem. Rev.* **122**, 1485–1542 (2022).
18. Zhu, Y. et al. Functionality-directed regio- and enantio-selective olefinic C-H functionalization of aryl alkenes. *Chem. Rec.* **23**, e202300012 (2023).
19. de Jesus, R., Hiesinger, K. & van Gemmeren, M. Preparative scale applications of C–H activation in medicinal chemistry. *Angew. Chem. Int. Ed.* **62**, e202306659 (2023).
20. Davies, H. M. L. & Manning, J. R. Catalytic C-H functionalization by metal carbenoid and nitrenoid insertion. *Nature* **451**, 417–424 (2008).
21. Davies, H. M. L. & Morton, D. Guiding principles for site selective and stereoselective intermolecular C-H functionalization by donor/acceptor rhodium carbenes. *Chem. Soc. Rev.* **40**, 1857–1869 (2011).
22. Che, C.-M., Lo, V. K.-Y., Zhou, C.-Y. & Huang, J.-S. Selective functionalisation of saturated C-H bonds with metalloporphyrin catalysts. *Chem. Soc. Rev.* **40**, 1950–1975 (2011).
23. He, Y. et al. Recent advances in transition-metal-catalyzed carbene insertion to C-H bonds. *Chem. Soc. Rev.* **51**, 2759–2852 (2022).
24. Zhang, Q., Wu, L.-S. & Shi, B.-F. Forging C-heteroatom bonds by transition-metal-catalyzed enantioselective C-H functionalization. *Chem* **8**, 384–413 (2022).
25. Godula, K. & Sames, D. C-H bond functionalization in complex organic synthesis. *Science* **312**, 67–72 (2006).
26. Cernak, T., Dykstra, K. D., Tyagarajan, S., Vachal, P. & Krska, S. W. The medicinal chemist's toolbox for late stage functionalization of drug-like molecules. *Chem. Soc. Rev.* **45**, 546–576 (2016).
27. Guillemard, L., Kaplaneris, N., Ackermann, L. & Johansson, M. J. Late-stage C-H functionalization offers new opportunities in drug discovery. *Nat. Rev. Chem.* **5**, 522–545 (2021).
28. Liao, K., Negretti, S., Musaev, D. G., Bacsa, J. & Davies, H. M. L. Site-selective and stereoselective functionalization of unactivated C-H bonds. *Nature* **533**, 230–234 (2016).
29. Liao, K. et al. Site-selective and stereoselective functionalization of non-activated tertiary C-H bonds. *Nature* **551**, 609–613 (2017).
30. Fu, J., Ren, Z., Bacsa, J., Musaev, D. G. & Davies, H. M. L. Desymmetrization of cyclohexanes by site- and stereoselective C-H functionalization. *Nature* **564**, 395–399 (2018).

31. Gensch, T., James, M. J., Dalton, T. & Glorius, F. Increasing catalyst efficiency in C-H activation catalysis. *Angew. Chem. Int. Ed.* **57**, 2296–2306 (2018).
32. Salazar, C. A. et al. Tailored quinones support high-turnover Pd catalysts for oxidative C-H arylation with O_2. *Science* **370**, 1454–1460 (2020).
33. Das, S., Incarvito, C. D., Crabtree, R. H. & Brudvig, G. W. Molecular recognition in the selective oxygenation of saturated C-H bonds by a dimanganese catalyst. *Science* **312**, 1941–1943 (2006).
34. Jia, C. et al. Efficient activation of aromatic C-H bonds for addition to C-C multiple bonds. *Science* **287**, 1992–1995 (2000).
35. Zbieg, J. R., Yamaguchi, E., McInturff, E. L. & Krische, M. J. Enantioselective C-H crotylation of primary alcohols via hydrohydroxyalkylation of butadiene. *Science* **336**, 324–327 (2012).
36. Tsutsui, H. et al. Dirhodium(II) tetrakis *N*-tetrafluorophthaloyl-(*S*)-*tert*-leucinate]: an exceptionally effective Rh(II) catalyst for enantiotopically selective aromatic C-H insertions of diazo ketoesters. *Tetrahedron Asymmetry* **14**, 817–821 (2003).
37. Davies, H. M. L. & Liao, K. Dirhodium tetracarboxylates as catalysts for selective intermolecular C-H functionalization. *Nat. Rev. Chem.* **3**, 347–360 (2019).
38. Thu, H.-Y. et al. Highly selective metal catalysts for intermolecular carbenoid insertion into primary C-H bonds and enantioselective C-C bond formation. *Angew. Chem. Int. Ed.* **47**, 9747–9751 (2008).
39. Liao, K. et al. Design of catalysts for site-selective and enantioselective functionalization of non-activated primary C-H bonds. *Nat. Chem.* **10**, 1048–1055 (2018).
40. Zhang, R. K. et al. Enzymatic assembly of carbon-carbon bonds via iron-catalysed sp^3 C-H functionalization. *Nature* **565**, 67–72 (2019).
41. Dydio, P. et al. An artificial metalloenzyme with the kinetics of native enzymes. *Science* **354**, 102–106 (2016).
42. Greule, A., Stok, J. E., De Voss, J. J. & Cryle, M. J. Unrivalled diversity: the many roles and reactions of bacterial cytochromes P450 in secondary metabolism. *Nat. Prod. Rep.* **35**, 757–791 (2018).
43. Lukowski, A. L. et al. C-H hydroxylation in paralytic shellfish toxin biosynthesis. *J. Am. Chem. Soc.* **140**, 11863–11869 (2018).
44. Yang, Y. & Arnold, F. H. Navigating the unnatural reaction space: directed evolution of heme proteins for selective carbene and nitrene transfer. *Acc. Chem. Res.* **54**, 1209–1225 (2021).
45. Wang, J.-C. et al. Highly enantioselective intermolecular carbene insertion to C-H and Si-H bonds catalyzed by a chiral iridium(III) complex of a D_4-symmetric Halterman porphyrin ligand. *Chem. Commun.* **48**, 4299–4301 (2012).
46. Wang, J. C., Zhang, Y., Xu, Z.-J., Lo, V. K.-Y. & Che, C.-M. Enantioselective intramolecular carbene C-H insertion catalyzed by a chiral iridium(III) complex of D_4-symmetric porphyrin ligand. *ACS Catal.* **3**, 1144–1148 (2013).
47. Liu, Z. et al. Assembly and evolution of artificial metalloenzymes within *E. coli* Nissle 1917 for enantioselective and site-selective functionalization of C-H and C=C bonds. *J. Am. Chem. Soc.* **144**, 883–890 (2022).
48. Anding, B. J., Dairo, T. O. & Woo, L. K. Reactivity comparison of primary aromatic amines and thiols in E-H Inertion reactions with diazoacetates catalyzed by iridium(III) tetratolylporphyrin. *Organometallics* **36**, 1842–1847 (2017).
49. Dairo, T. O. & Woo, L. K. Scope and mechanism of iridium porphyrin-catalyzed S-H insertion reactions between thiols and diazo esters. *Organometallics* **36**, 927–934 (2017).
50. Anding, B. J., Ellern, A. & Woo, L. K. Olefin cyclopropanation catalyzed by iridium(III) porphyrin complexes. *Organometallics* **31**, 3628–3635 (2012).
51. Balhara, R., Chatterjee, R. & Jindal, G. A computional approach to understand the role of metals and axial ligands in artificial heme enzyme catalyzed C-H insertion. *Phys. Chem. Chem. Phys.* **23**, 9500–9511 (2021).
52. Key, H. M., Dydio, P., Clark, D. S. & Hartwig, J. F. Abiological catalysis by artificial haem proteins containing noble metals in place of iron. *Nature* **534**, 534–537 (2016).
53. Suematsu, H. & Katsuki, T. Iridium(III) catalyzed diastereo- and enantioselective C-H bond functionalization. *J. Am. Chem. Soc.* **131**, 14218–14219 (2009).
54. Guptill, D. M. & Davies, H. M. L. 2,2,2-Trichloroethyl aryldiazoacetates as robust reagents for the enantioselective C-H functionalization of methyl ethers. *J. Am. Chem. Soc.* **136**, 17718–17721 (2014).
55. Xu, B., Li, M.-L., Zuo, X.-D., Zhu, S.-F. & Zhou, Q.-L. Catalytic asymmetric arylation of α-aryl-α-diazoacetates with aniline derivatives. *J. Am. Chem. Soc.* **137**, 8700–8703 (2015).
56. Zhu, D.-X., Xia, H., Liu, J.-G., Chung, L. W. & Xu, M.-H. Regiospecific and enantioselective arylvinylcarbene insertion of a C-H bond of aniline derivatives enabled by a Rh(I)-diene catalyst. *J. Am. Chem. Soc.* **143**, 2608–2619 (2021).
57. Li, Z. et al. Construction of C-C axial chirality via asymmetric carbene insertion into arene C-H bonds. *Angew. Chem. Int. Ed.* **60**, 25714–25718 (2021).
58. Yuan, S., Li, S.-Y., Zhao, X.-M., Lin, Y.-Z. & Zheng, S.-C. Enantioselective alkylation of primary C(sp^3)–H bonds in *N*-methyl tertiary amine enabled by iridium complex of axially chiral *β*-aryl porphyrins. *J. Am. Chem. Soc.* **147**, 51–56 (2025).
59. Chen, G., Arai, K., Morisaki, K., Kawabata, T. & Ueda, Y. Dirhodium-catalyzed chemo- and site-selective C-H amidation of *N*,*N*-dialkylanilines. *Synlett* **32**, 728–732 (2021).

Acknowledgements

This work is supported by the Hong Kong Research Grants Council General Research Fund (17302020, (C.-M.C.)), the National Key R&D Program of China (2017YFE0190100, (C.-M.C.)), the National Natural Science Foundation of China (NSFC 91856203, (C.-M.C.), 21472216, (Z.-J.X.) and 52173014, (G.-L.L.)), and the CAS-Croucher Funding Scheme for Joint Laboratories (C.-M.C.).

Author contributions

C.-M.C. conceived the project and directed the research. Z.-J.X. designed the experimental studies. Z.-R.L., K.Z., Y.-J.W., and Z.-J.X. carried out the reactions. L.-L.W. performed DFT calculations. G.-L.L. carried out the GPC and corresponding analysis of polymer. H.-Y.W. carried out the mass spectrum analysis. X.-L.W. carried out the HPLC analysis of the chiral products. K.-H.L. carried out the X-ray crystal structure analysis. C.-M.C. and Z.-J.X. wrote the manuscript.

Competing interests

The authors declare no competing interests.

Additional information

Supplementary information The online version contains supplementary material available at https://doi.org/10.1038/s41467-025-58316-1.

Correspondence and requests for materials should be addressed to Zhen-Jiang Xu or Chi-Ming Che.

Peer review information *Nature Communications* thanks Jun-Fang Gong, Xiao-Wei Liang and Tatsuya Uchida for their contribution to the peer review of this work. A peer review file is available.